Design of Test Bench Apparatus and Preliminary Weight Reduction Strategy for an Active Knee Prosthesis

by

Jacky H. Lau

SUBMITTED TO THE DEPARTMENT OF MECHANICAL ENGINEERING IN PARTIAL FULLFILLMENT OF THE REQUIREMENTS FOR THE DEGREE OF

BACHELOR OF SCIENCE IN MECHANICAL ENGINEERING
AT THE
MASSACHUSETTS INSTITUTE OF TECHNOLOGY

JUNE 2011

Signature of Author: ____________________
Department of Mechanical Engineering
May 17, 2011

Certified by: ____________________
Hugh M. Herr
Associate Professor, Media Arts and Sciences
Associate Professor, MIT-Harvard Division of Health Sciences and Technology
Director of Biomechatronics Group
Thesis Supervisor

Accepted by: ____________________
John H. Lienhard V
Collins Professor of Mechanical Engineering
Chairman, Undergraduate Thesis Committee

Design of Test Bench Apparatus and Preliminary Weight Reduction Strategy for an Active Knee Prosthesis

by

Jacky H. Lau

Submitted to the Department of Mechanical Engineering on May 17, 2011 in Partial Fulfillment of the Requirements for the Degree of Bachelor of Science in Mechanical Engineering

ABSTRACT

This thesis presents the design and structural analyses of an experimental test bench for the characterization of an active biomimetic knee prosthesis currently being developed by the Biomechatronics research group at MIT Media Laboratory. Finite element analysis (FEA) is conducted to determine the maximum stress and material deflections of three principle components of the test bench and to verify their structural integrity. In addition, FEA is performed on the chassis of the active knee prosthesis when subjected to the expected loads associated with walking. The simulation results verify that the active prosthetic do not expect structural failure during level ground walking trials with above knee amputee participants. Finally, an empirical weight reduction strategy for the active knee is proposed and analyzed. This strategy aims to reduce distal leg mass which contributes to the overall energetic demands of amputee walking. FEA on the modified active knee prosthesis chassis validate the strategy modifications while maintaining the original design feature constraints.

Thesis Supervisor: Hugh M. Herr
Title: Associate Professor, Media Arts and Sciences Program
Associate Professor, MIT Harvard Division of Health Sciences and Technology
Director of Biomechatronics Group

Acknowledgements

I would like to thank Professor Hugh Herr and the rest of the Biomechatronics group at the MIT Media Lab for giving me the opportunity to work with and learn from them. My research experience at the Biomechatronics group strengthened my understanding of mechanical engineering principles and further enhanced my research abilities. I would also like to give a special thank you to my direct supervisor, Ernesto Martinez-Villalpando, for taking me under his wing and teaching me the "Biomech" way. In addition to mentoring my research at Biomechatronics, he also provided countless hours of revision and guidance for my work in this thesis.

I would also like to thank my previous research supervisors and mentors Lifeng Wang, Mary Boyce, Lawrence Malagaya, and others for their supervision and guidance which helped develop my research skills and understanding of mechanical engineering concepts.

Finally, I would like to thank my family for their continual support throughout my education process and beyond.

Table of Contents

List of Figures

List of Tables

1. Introduction

Above-knee (AK) amputees, often referred as transfemoral amputees, experience several gait pathologies. Among the most important are asymmetric gait patterns, slower gait speeds, and elevated metabolic costs of ambulation as compared to intact subjects (Johansson et al, 2005). Despite the advantages currently available prostheses possess, their technologies are limited and cannot fully restore intact limb functionality (James, 1973: Huang et al 2000).

The Biomechatronics research group at MIT's Media Laboratory has been developing a novel biomimetic active knee prosthesis that is capable of reproducing knee biomechanics in order to improve amputee locomotion (Martinez-V. et al, 2008*, 2009). This research group currently has two active knee prototypes in development, referred as Revision_0 and Revision_1. Revision_0 is in a later stage of development undergoing human trials that evaluate its clinical impact on AK amputees. Revision_1 is in early stages of development, as it requires going through a series of "*test-bench*" evaluations. These evaluations will ensure that the prototype meets functional design specifications. Furthermore, they will provide a setting for mechanical system characterization and a basis for control algorithm development prior to conducting amputee tests. In order to conduct the *test-bench* evaluations for the active knee prostheses, a custom apparatus is required. In this thesis, I present the design and structural analysis of the main components of the test bench that accommodate the Revision_1 prototype.

The active knee prosthesis being developed is capable of providing net positive power output at the knee joint, which most of the conventional knee prostheses cannot provide. This feature of the active knee is hypothesized to reduce amputees' higher metabolic costs of walking and increased locomotion fatigue associated with the lack of proper mobility. In addition to positive power output, a key consideration for the active prosthesis design is weight. Any unnecessary distal mass corresponding to the prosthesis can contribute to an increase in the energetic demand to the amputee (Browning, 2007). In this thesis, I present a weight reduction strategy on the chassis of Revision_1 in order to minimize weight and help improve the impact on amputee ambulation.

The main work for this thesis is described in chapters 2 and 3. In chapter 2, I describe the design and structural analyses of three main components of the test bench apparatus that will be used to evaluate the active knee prosthesis Revision_1. In chapter 3, I propose a weight reduction strategy for the active knee, evaluate the structural integrity of the resulting design and confirm it meets established design constraints. In the final chapter, I present concluding remarks of the thesis work and make some suggestions for future work.

2. Test Bench Apparatus for Active Knee Prosthesis

An experimental test bench apparatus was developed in order to help evaluate the performance and capabilities of the active knee prosthesis prior to conducting amputee testing trials. This apparatus will enable a system characterization for a full model description of the physical actuators of the prosthesis and will help provide system model parameters for control algorithm development.

The biomimetic active knee prosthesis being developed at MIT's Biomechatronics group is a motorized device capable of reproducing knee biomechanics during level ground walking. This prosthesis has a novel electromechanical design that incorporates a dual series elastic actuator (SEA) system that enables the control of the knee joint. The SEAs are composed of a DC motor connected to a linear ballscrew transmission system via a belt drive. The two SEAs are unidirectional and independently actuate the state of a linear carriage that directly connects to the knee joint via a cable drive. Each SEA independently controls the flexion and extension of the knee joint. Figure 2-1 shows the solid model of the Revision_1 active knee prosthesis.

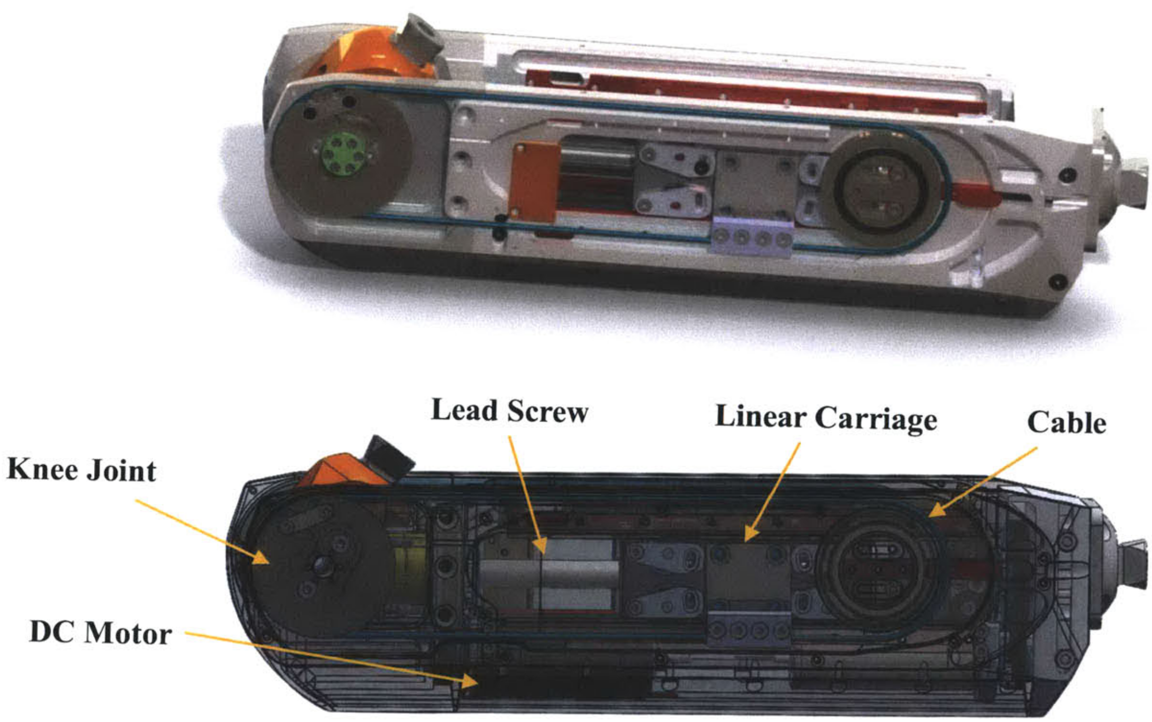

Figure 2-1: (A) Rendered solid model of Revision_1 active knee prosthesis. (B) Solid model with key components labeled.

The full assembly of the test bench apparatus including the Revision_1 of the active knee prosthesis is shown in Figure 2-2.

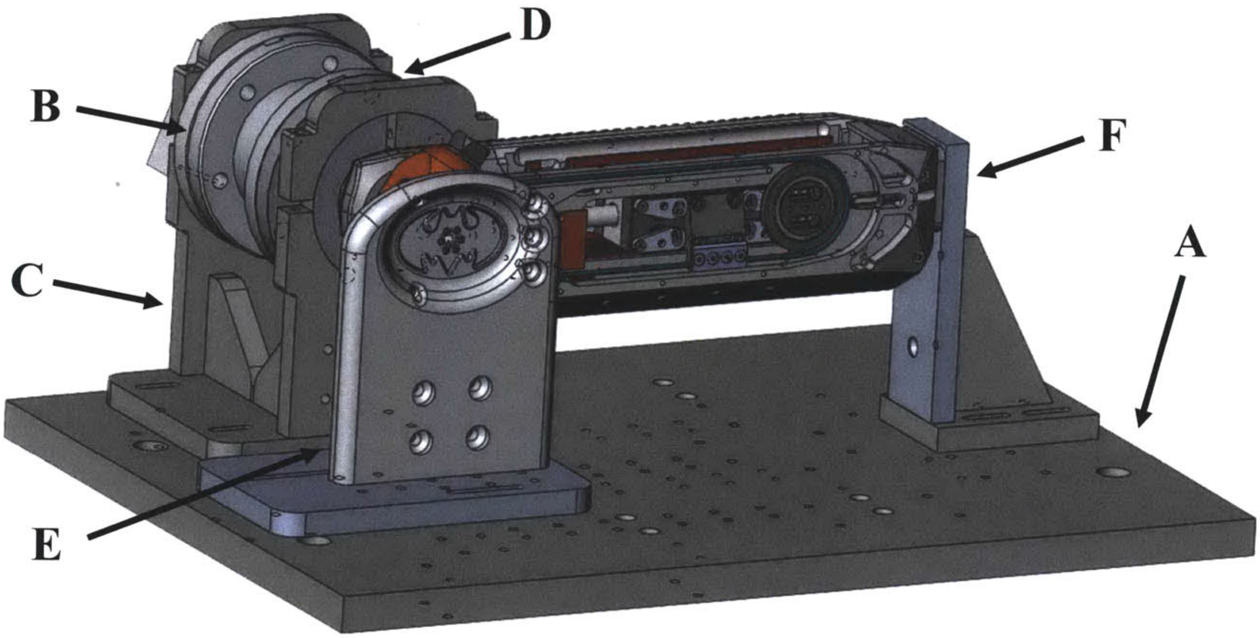

Figure 2-2: Solid model of the test bench assembly with Revision_1 active knee prosthesis. The main test bench components are highlighted: the support base (A), the torque sensor (B), the torque sensor mount (C), the torque sensor adapter (D), the joint lateral mount (E), and the distal mount(E).

The test bench apparatus has six main components: a support base, a torque sensor, a torque sensor mount, a torque sensor adapter, a joint lateral mount, and a distal mount.

The ***support base*** is made of three-quarters inch 1020 steel and serves as a rigid base for the test bench apparatus. It possesses a pattern of 10-24 tapped holes that allow the attachment of the torque sensor mount, the distal mount, and the joint lateral mount.

The ***torque sensor*** used for the system characterization of the active knee prosthesis is the Futek TFF600 Reaction Torque Sensor. The purpose of this sensor is to measure the output torque generated by the knee joint during the testing procedures.

The ***torque sensor mount*** serves as a rigid mount to securely fix one end of torque sensor to the test bench apparatus. It also helps attach the other end of the torque sensor to the knee joint through an eccentric circular clamp. This feature helps adjusts the alignment of the torque sensor to precisely mate with the knee prosthesis.

The ***torque sensor adapter*** has two main functions:

1) Fully support the torque sensor while maintaining the proper axial alignment with the prosthetic knee.
2) Enable the transmission of torque from the knee joint to be fully sensed by the torque sensor

The ***joint-lateral mount*** provides supports to the contra-lateral side of the prosthetic knee joint as it assists in the load bearing of the prosthesis. Complementing the function of the torque sensor mount, this part helps assure a rigid support of the knee joint during the characterization testing procedures.

The ***distal mount*** attaches to the bottom face of the knee prosthesis, providing a rigid support to devices' distal end. This part ensures a fully constrained mounting of the knee prosthesis during the characterization testing procedures. This mount shares the load of the prosthesis weight and minimizes knee deflection as during the active testing of the knee device where torque is generated by the knee joint.

For this thesis, I designed the torque sensor adapter as well as the lateral and distal mounts that will fully support the active knee prosthesis. In the following sections, the design and mechanical structural analysis (via finite element analyses) of these three components is described. The prevention of material yielding and deflection failure were the primary values focus of the finite element analyses (FEA). All three parts were made of 6061 Aluminum with a yield stress of ~55 MPa (Matweb, 2011). For the analyzed parts the maximum deflection should follow Equation 2-1 which correlates to an acceptable stiffness to prevent excess vibrations during testing. (AISC, 1989)

$$maximum\ deflection = \frac{span}{360} \tag{2-1}$$

2.1 Torque Sensor Adapter

2.1.1 Design Criteria and Part Description

The design of the torque sensor adapter must satisfy three important criteria:

1) Mate and attach to the Futek TFF600 Reaction Torque Sensor.
2) Mate and attach to the knee joint of the prosthesis guaranteeing the transmission of torque generated by the knee to the torque sensor.
3) Structurally withstand the torque generated by the knee joint which corresponds to a maximum stress level less than the yield stress of the material while supporting the knee joint.

The torque sensor adapter is made of 6061 Aluminum alloy. The full detailed drawings can be seen in Appendix A. Figure 2-2 shows the solid model of the torque sensor adapter from two different views with critical features labeled.

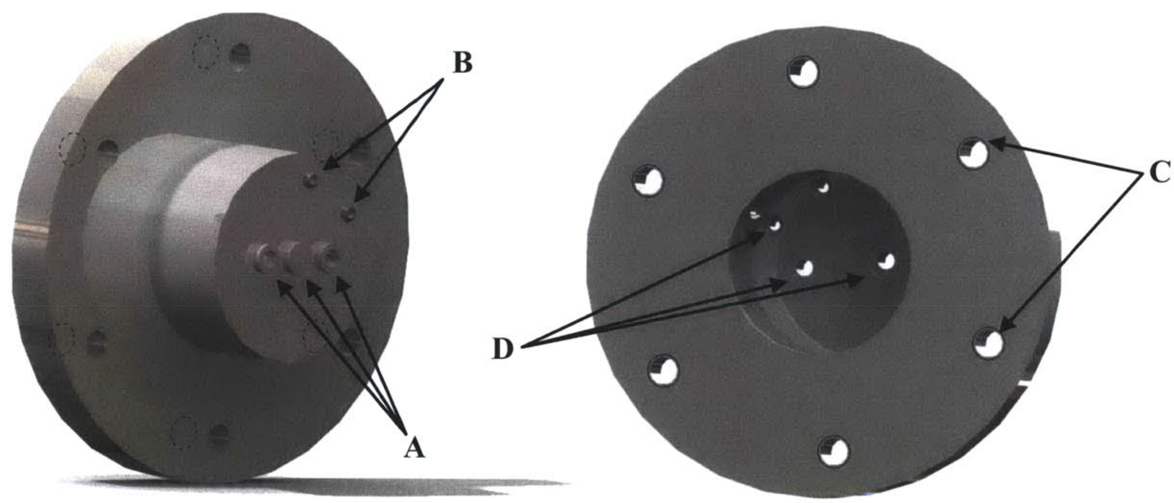

Figure 2-3: The image on the left shows the torque sensor adapter with the portion that attaches to the knee joint shown. The reverse counter bore (A) and reverse countersink (B) features allow the torque sensor adapter to mate to the knee joint. The image of the right is the torque sensor adapter with the portion which attaches to the torque sensor shown. Tapped hole-features (C) allow the torque sensor adapter to attach to the torque sensor and the through-hole (D) features allow for the attachment of the torque sensor adapter to the knee joint.

In order to satisfy the first and second criteria, solid models of the torque sensor and Revision_1 active knee prosthesis were referenced when designing the torque sensor adapter. The torque sensor adapter has six 5/16-24 tapped holes in a circular pattern, labeled (C) in Figure 2-3. These mating holes correspond to the through-hole support features found on the Futek torque sensor that allow it to be bolted to the custom torque sensor adapter. The reverse counter bore and reverse countersink features, labeled (A) and (B) respectively in Figure 2-3, allow the part to mate with the knee joint of prosthesis. The inner surface of torque sensor contains through-hole features, labeled (D) on Figure 2-3, which allow the attachment of the torque sensor adapter to the joint of the active prosthesis. The specific tolerance criteria and geometric cuts in this part (specifically the reverse countersink and reverse counter bore features on one its faces), required us to get the part manufactured by a machining house outside MIT. (The part was contour milled out of 6061 Aluminum alloy.)

The third design criterion was verified using finite element analysis (FEA) to determine the von mises stress distribution of the part and confirming that the maximum stress the part experiences will not exceed the yield stress of the material (~55 MPa for 6061 Aluminum Alloy) (Matweb 2011).

2.1.2 Analysis and Results

In order to perform the necessary FEA to verify the structural integrity of the torque sensor adapter, several assumptions needed to be made. First is the expected load the part will experience. Second is the direction of the load. Third, are the fixed geometries of the solid model. To determine the expected maximum load the torque sensor adapter will experience during the testing procedures, the experimental torque values found while performing the initial characterization procedures for first active knee prosthesis prototype (Revision_0) were used. These tests were performed in a very similar test bench apparatus designed to accommodate the Revision _0 device. The maximum torque readings captured by the Futek TFF600 sensor during the basic loading experiments with Revision_0 did not exceed 45 Nm.

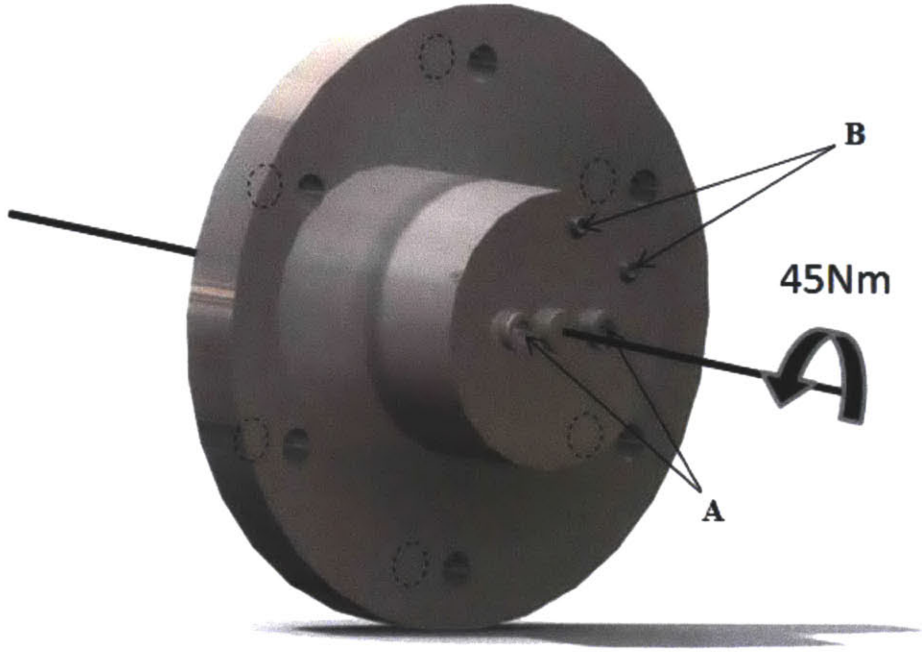

Figure 2-4: Finite element analysis set up for torque sensor adapter. (A) Counter bore through-holes and (B) countersunk through-holes are set as the fixed geometry. A torque of 45Nm is applied axial to the part and the material property for 6061 Aluminum alloy was chosen for the simulation.

The direction of the torque applied for the analysis was around the central axis of the part as illustrated in Figure 2-4. The through-hole features of which serve as attachment features for the knee joint were set as the fixed geometries. The reason the tapped holes that attach to and support the torque sensor were not chosen as fixed geometries as these features will have a relative motion as the torque sensor captures the effective torsional moments applied by the active knee joint.

The resulting stress distribution in the torque sensor adapter part after performing the FEA with the conditions previously depicted in Figure 2-5. The highest level of stress the part experiences is approximately ~44 MPa which does not exceed the yield stress of ~55MPa, corresponding to the yield stress of the material (Al 6061).

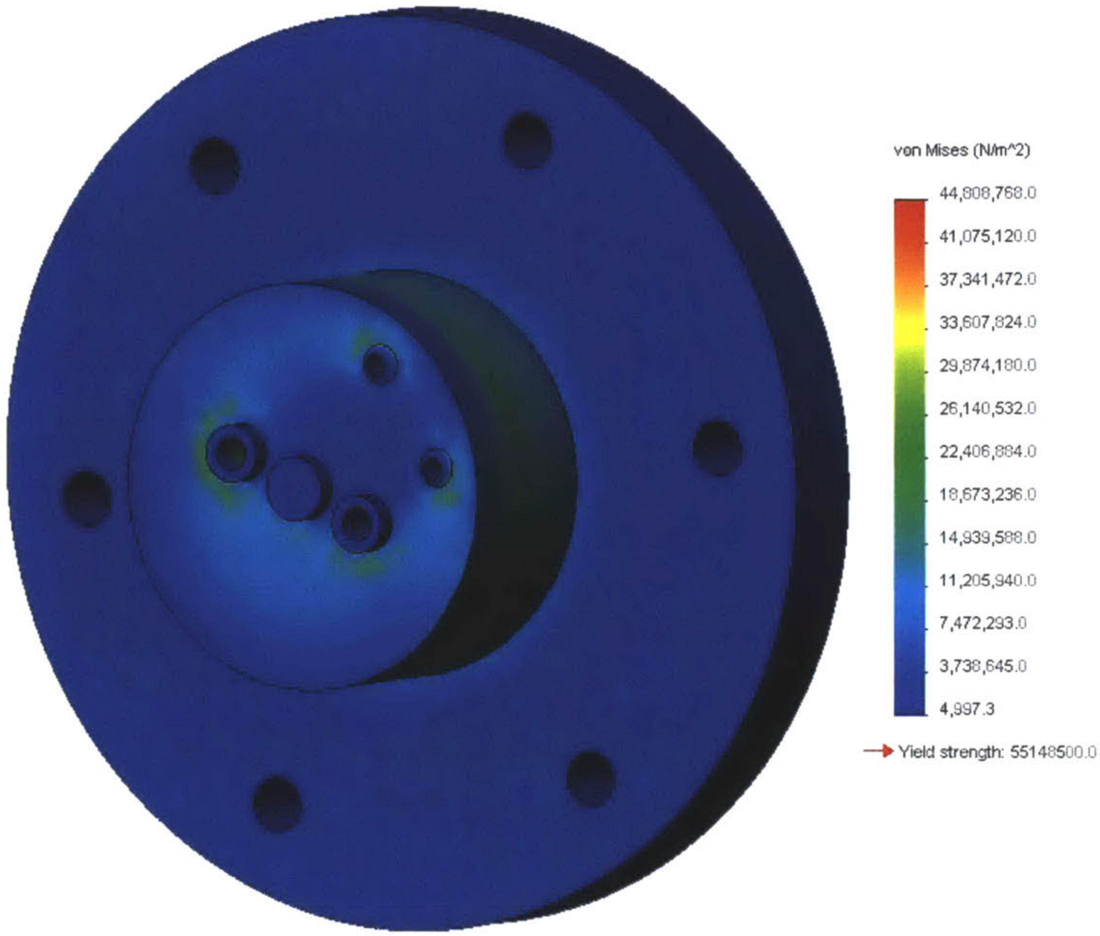

Figure 2-5: FEA, von-mises stress distribution result for the torque sensor adapter.

2.2 Joint Lateral Mount

2.2.1 Design Criteria and Part Description

Another crucial component of the test bench apparatus is the joint lateral mount. This part should include mounting features for a digital encoder that senses knee angle. Moreover, this part should be structurally rigid in order to enable fixing the Revision_1 active knee prosthesis to the support base during characterization experiments. This support is also meant to reduce mechanical vibrations during the characterization process. Figure 2-6 shows the rendered image of the joint lateral mount system with a front and back view and main features labeled.

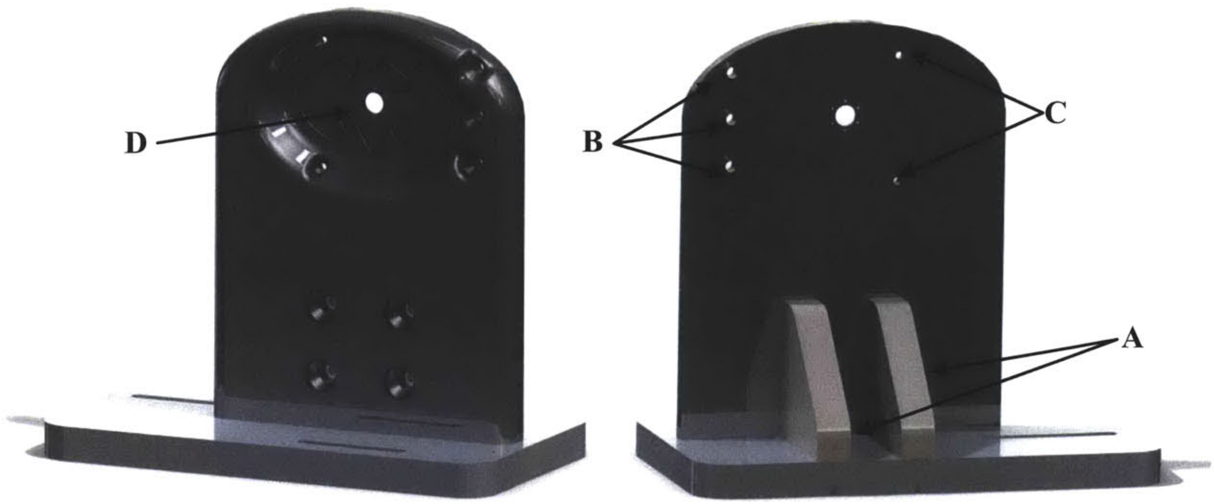

Figure 2-6: The image on the left shows the front of the joint lateral mount system and the image on the right shows the back of the joint lateral mount system.

The joint lateral mount features six tapped holes for M1.2 x 0.25 screws, labeled (D) in Figure 2-6, arranged in a circular pattern which complements the through-hole features of the digital encoder sensor. This portion of the knee-mount has a thickness of 0.06 inches, corresponding to the thickness as the prosthesis's side plate that supports the encoder during. This feature is of importance to ensure that the part will be at the correct distance from the encoder to ensure functionality during the amputee user studies. The joint lateral mount attaches to the frame of the knee prosthesis chassis through three M4 countersink screws and two M2.5 countersink screws. Three reverse countersink features, labeled (B) in Figure 2-6, are designed to mate to the chassis of the knee prosthesis and two additional through-holes, labeled (C) in Figure 2-6, provide the means to attach the knee-mount to the active knee prosthesis. The detailed engineering drawings of the part can be found in Appendix A.

In order to provide a rigid structure to the joint lateral mount, two wedges, labeled (A) in Figure 2-6, were machined to attach the joint lateral mount to a base plate which is then bolted to the bottom of the test bench base. The wedges and the base plate are made of 6061 Aluminum Alloy. These parts are half inch thick. The criterion for determining the rigidity of the system will be determined using a finite element analysis of the system and determining the maximum deflection of the part. The maximum deflection of the part should not exceed the span of the part divided by 360 which is the stiffness criteria used in design to reduce vibrations from walking (AISC, 1989). This gives a maximum deflection limit of 4.23×10^{-4} m.

2.2.2 Analysis and Results

For the lateral mount I analyzed the maximum deflection and maximum stress of the joint lateral mount due to expected loading during testing procedures. Under the assumption that each of the three main weight bearing parts of the apparatus will equally share the knee's weight of approximately 29 N, the value of 30 N vertical load was employed for FEA. This load was applied to the reverse countersink features of the knee-mount, labeled (B) in Figure 2-6, which assumes that each feature will sustain 10N for a total of 30 N. This part does not attach to the torque generating knee joint, the possible torque on the part was neglected. Next, the fixed geometries and connectors must be established in the assembly. The bottom support plate is defined as fix because it is bolted to a solid steel base. The wedges were attached with 1/4-20 bolt connectors. The whole assembly was made of half inch 6061 Aluminum Alloy.

Figure 2-7 shows the expected displacement of the part under 10N of force being applied to three bolt features. The maximum displacement of any point is on the magnitude of 10^{-6} m. This magnitude of deflection is smaller than the deflection limit of 4.23×10^{-4} m. However, this result assumes that the torque generated at the torque will not affect the joint lateral mount and that the torque sensor adapter and the distal mount will experience all of the torque reaction moments. To compensate for this assumption, the total assumed load applied to the knee-mount was approximately the entire weight of the prosthesis rather than a portion of the weight of the prosthesis. The maximum stress in the part was found to be ~3 MPa which is much smaller than the yield stress of 6061 Aluminum (yield stress ~ 55MPa). The finite element results depicting the stress distribution of the joint lateral mount can be found in Appendix B.

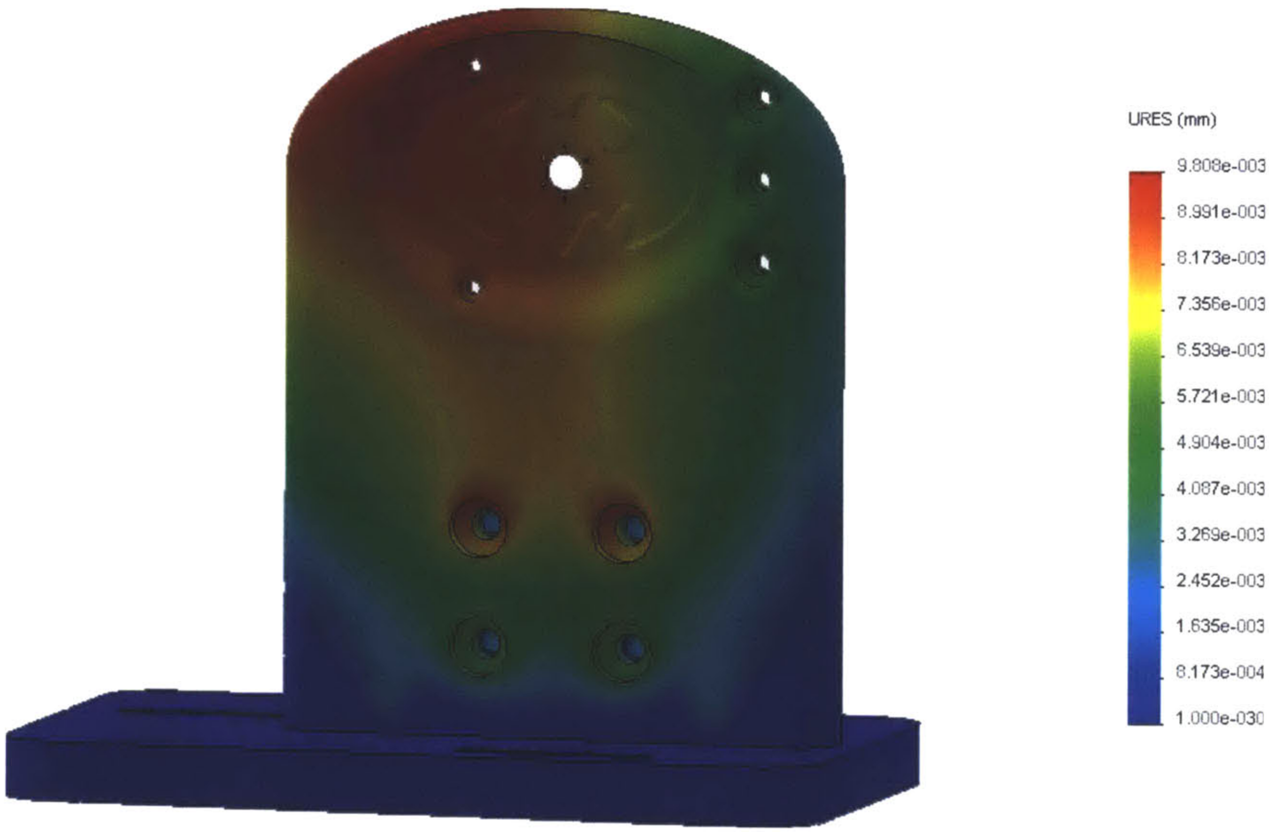

Figure 2-7: Finite element analysis showing the displacement of the joint lateral mount wedge system.

2.3 Distal Mount

2.3.1 Design Criteria and Part Description

The primary function is to rigidly mount the distal end of the active knee prosthesis to the test bench. The criterion is quantified by having a maximum deflection of less than 3.97 x 10^{-4} m which correlates to the span of the part divided by 360 (AISC, 1989). The rendered images of the distal mount system are shown in Figure 2-8 with main features labeled. The distal mount is bolted to a wedge, labeled (A) in Figure 2-8, and a base plate, labeled (C) in Figure 2-8, using four M5 countersink screws. The wedge is bolted to the base plate using two M5 countersink screws. The distal mount base plate is bolted to the steel base plate of the test bench apparatus using four 10-24 screws. The distal mount attaches to the knee prosthesis through four M6 countersink screws in a custom symmetric hole-pattern. The reverse countersink features on the front of the distal mount, labeled (B) in Figure 2-8, mates with the distal plate adapter of the active knee prosthesis. This standard plate connects to commercial prosthetic feet.

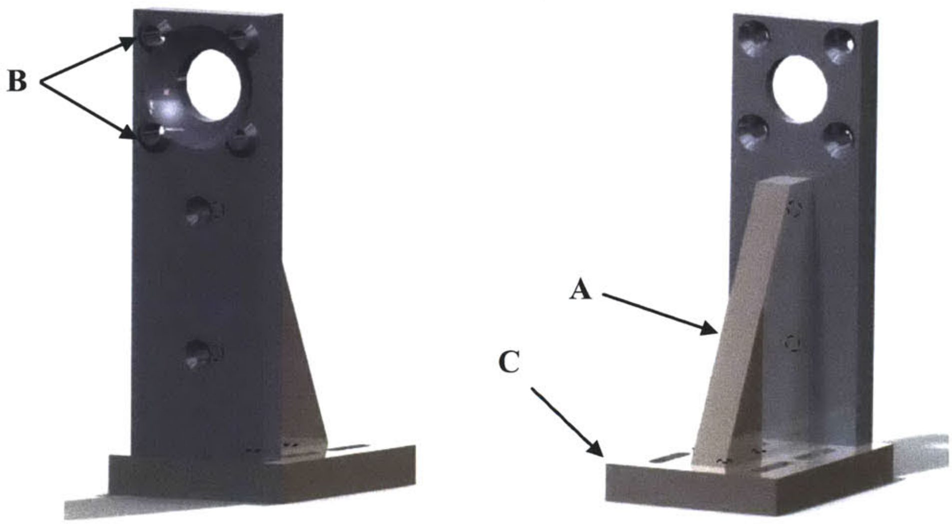

Figure 2-8: The image on the left shows the front of the distal-mount system and the image on the right shows the back of the distal-mount system.

2.3.2 Analysis and Results

In order to determine the maximum deflection and maximum stress of the distal-mount during the characterization process, the expected maximum force must be derived. Using the maximum torque at the knee joint to be 45 Nm, the expected force at the distal mount can be determined using the length of the knee prosthesis. Incorporating a safety factor of two, the expected force of 300 N was derived using Equation 2-2 using the values found in Table 2-1.

Parameter	Value
τ_{max}	45 Nm
L_{knee}	0.305 m
S_{factor}	2

Table 2-1: Parameter values for estimating the expected force the distal mount will experience.

$$F_{expected} = \frac{\tau_{max}}{L_{knee}} S_{factor} = \frac{(45\ Nm)}{(0.305\ m)}(2) = 296\ N \approx 300N \tag{2-2}$$

The 300 N load was applied to the reverse countersink features, labeled (B) in Figure 2-8, and the force was applied upwards, normal from the base. The base plate was assumed to be fixed and the bolt connectors were applied according to the part description in the previous text. All the parts were given material properties of 6061 Aluminum Alloy.

Figure 2-9 shows the FEA results for the distal mount. The results of this analysis reveal that the order of magnitude of the greatest displacement is in the vicinity of 3 x 10^{-5} m. This value is less than the maximum deflection limit of 3.97 x 10^{-4} m for the material employed. Moreover, a stress analysis was also performed to ensure that the part will not yield due to excessive loads. The greatest points of stress was found to be on the order of 13 MPa which is approximately four times less than the yield stress of 6061 Aluminum Alloy (yield stress of ~55 MPa). The finite element results depicting the stress distribution of the distal mount can be found in Appendix B.

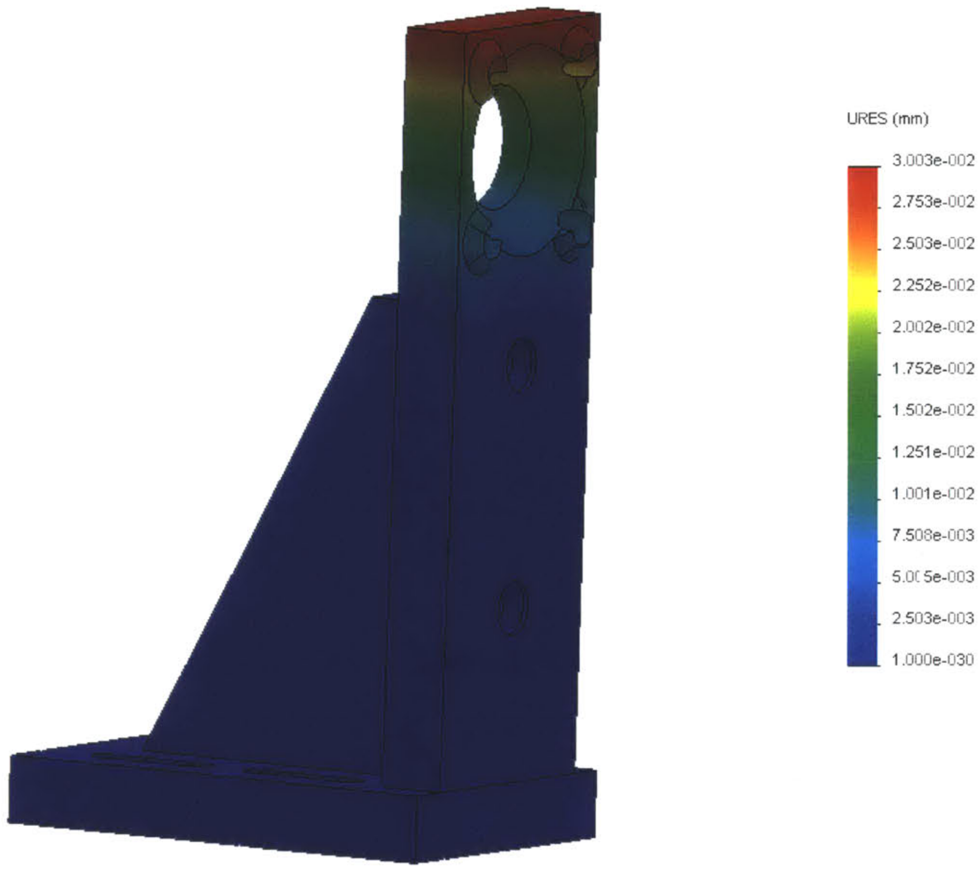

Figure 2-9: Finite element analysis showing the displacement of the distal mount wedge system.

3. Initial Weight Reduction Strategy

One of the main problems amputees face when using conventional knee prostheses is a higher metabolic cost of walking as compared to intact subjects. One particular reason associated with this problem is the inability of the prosthesis to fully replicate the biomechanical behavior of the intact joint. The lack of proper artificial joint function imposes larger demands on the hip musculature of the residual limb to stabilize the limb during locomotion. This derives in an increase of metabolic demand (Whittle, 2003). Furthermore, increase in metabolic costs during walking has also been associated with added distal mass in the limb (Browning, 2007). For this reason, having a prosthesis that is lightweight is critical to minimize burden on the residual limb and improve energetic efficiency of the amputee.

The design of the active knee prostheses under development at Biomechatronics research group (Martinez-V. et al, 2008; Martinez-V. and Herr, 2009) are capable of reproducing intact knee biomechanics, however their structural designs have not been optimized to a minimum weight. In this chapter I propose and analyze the effects of a weight reduction strategy for the active knee prosthesis Revision_1 while ensuring the original functional features and mating constraints were kept.

Several methods were considered as strategies to reduce the overall weight of the active knee prosthesis:

1) Substitute material of the knee prosthesis components
2) Material removal by thinning and/or creating hole-features
3) Optimal structural redesign of the prosthesis to efficiently take advantage of structural and functional components (i.e. improvement mating parts, reducing number of fasteners, etc.)

In this thesis, I explore an initial weight reduction strategy focusing on structural material reduction such that the already established mating features of the prosthesis remain intact.

For the implementation of the proposed strategy, material was removed from the structural chassis of the prosthesis. Actuator and transmission elements of the prosthesis were maintained with no modification. In order to determine if material removal did not compromise the structural integrity of the chassis beyond material yield limitations, a finite element analysis using SolidWorks® simulation was performed. This analysis was implemented using maximum loading values seen during walking. The results allowed us to determine the maximum stress distribution of the chassis in walking. If the chassis does not fail, which corresponds to the stress levels below the yield stress of the material, then a preliminary method of material will be implemented. This will be followed by another series of finite element testing until the stress distribution limit is reached which is defined by the onset of yielding in the assembly.

3.1 Finite Element Analysis of Revision_1 Active Knee Prosthesis

3.1.1 Methodology

A finite element analysis was performed on the main structural chassis of the active knee prosthesis. The analysis seeks to obtain what the expected maximum stress distribution in the prosthesis structure would be while walking on level ground. For this analysis, only the maximum vertical forces the chassis experiences were obtained from biological ground reaction forces (vertical component) seen during level ground walking at self-selected speed by an average male. The force was assumed to act axially along the length of the knee. The torsional components applied at the joint were not considered for this assessment. The entire load was assumed to be sustained by the knee chassis. After the initial stress distribution of the chassis through FEA, material was removed from the chassis to reduce weight. A second FEA was performed to verify that the chassis will structurally withstand yield or fracture.

3.1.2 Chassis Components .

Figure 3-1 shows the exploded view of the main structural components of Revision1 active knee prosthesis. The knee joint support (A) in Figure 3-1 is connected to each of the side support plates, (B) and (C), by three M4 countersink bolts. The base support (D) is connected to each of the side support plates by two M4 counter bore bolts. Finally, the adapter plate (E) is connected to the base plate by four M6 countersink screws. All of these components are made of 7075 Aluminum with a yield stress of approximately 103 MPa except for the distal adapter plate which is made of stainless steel with a yield stress of approximately 250 MPa (Matweb, 2011).

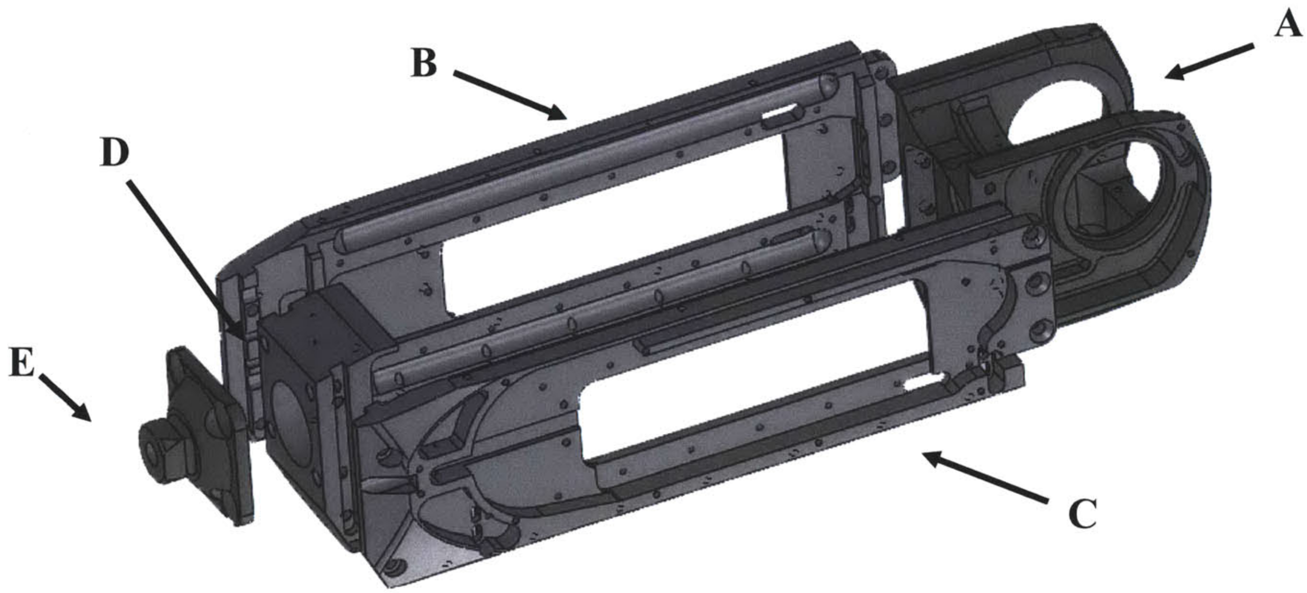

Figure 3 -1: Exploded view of the structural chassis components of Revision1 active knee prosthesis which includes five components: (A) knee joint support, (B) and (C) side supports, (D) base support, and (E) distal adapter plate.

3.1.3 Expected Forces from Walking

The amount of force exerted on the knee prosthesis can be determined by the reaction forces associated with level ground walking. The amount of ground reaction force is dependent on the walking speed or the cadence of the subject (Winter, 1991). Normalized values of ground reaction forces reported by Winter were used as a basis for this analysis. We assumed the maximum axial load on the knee prosthesis corresponds to the maximum vertical ground reaction force during fast level ground walking for a 250 lbs person. Figure 3-2 and Figure 3-3 show the average normalized vertical forces versus percentage of walking gait and average normalized horizontal forces versus percentage of walking-gait for a slow cadence. Figure 3-4 and Figure 3-5 shows the corresponding results for fast cadence.

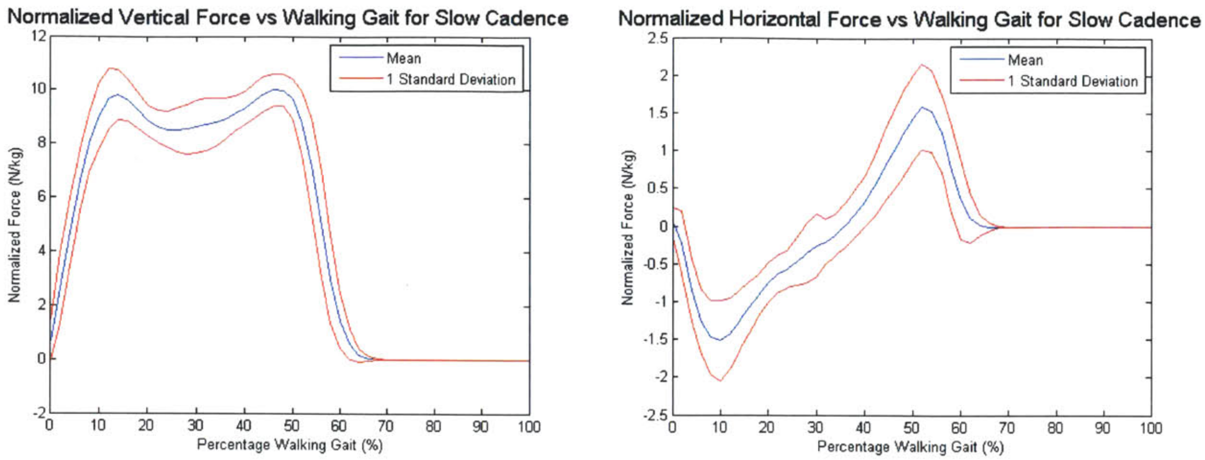

Figure 3-2 and 3-3: Normalized ground reaction force versus gait percentage for slow cadence walking. Left figure shows vertical forces and right figure shows horizontal forces.

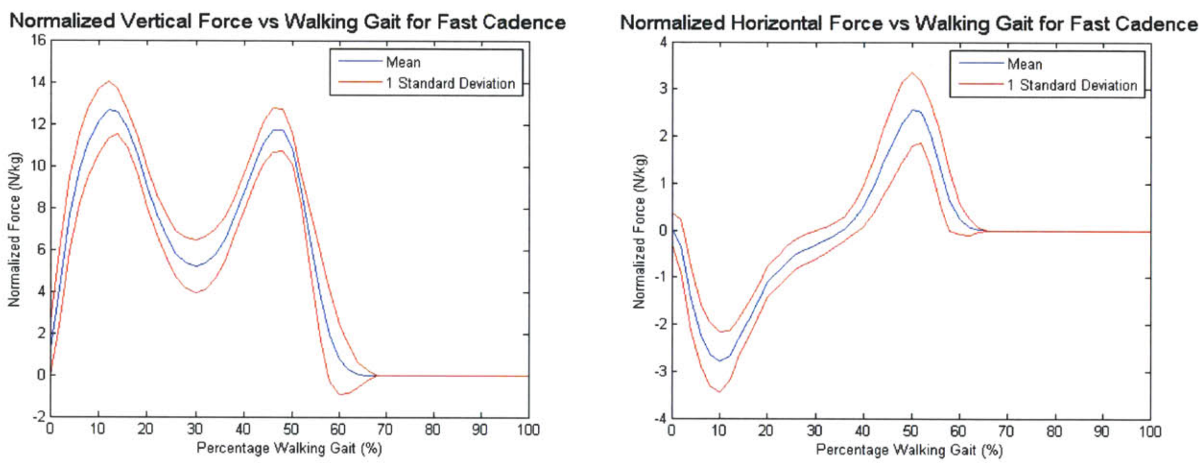

Figure 3-4 and 3-5: Normalized ground reaction force versus walking gait percentage for fast cadence walking. Left figure shows vertical forces and right figure shows the horizontal forces.

Faster cadence has a corresponding higher maximum vertical reaction force. The maximum force used for the finite element simulation will correspond to vertical force associated with fast cadence. The maximum vertical force found from the normalized data for a fast cadence was 12.67 N/kg with a standard deviation of 1.36 N/kg. After considering a safety factor of two, the normalized value used for the simulation was 30.78 N/kg. This value is approximately twice the maximum average vertical force plus two standard deviations. With an upper weight limit of a 250 lbs amputee patient, this corresponds to 114 kg which gives us an expected force of 3509 N with a safety factor of two included.

3.1.4 Force Load to Pressure Load

In order to get a more accurate simulation of the expected stress distribution, the force load was converted to a pressure load since the whole area does not experience the force of 3509N but rather distributed over the contact surface of the distal adapter plate. This assumption provides a more accurate distribution of the expected stresses along the structural chassis. Figure 3-6 highlights the area of the adapter plate where the pressure load was applied.

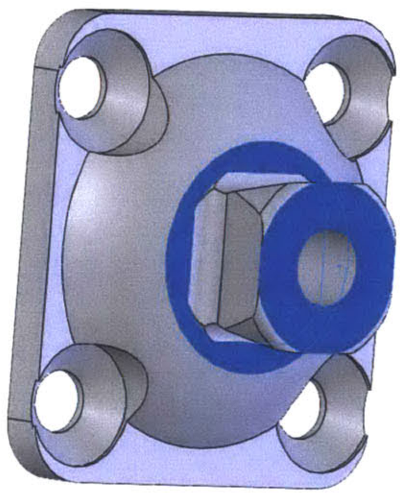

Figure 3 -6: Adapter plate on Revision1 chassis with the regions which experiences the maximum normal ground reaction force shaded in blue.

The shaded region represents the area of the knee distal adapter plate considered as the loading area. This plate connects to standard prosthetic components that allow the attachment of prosthetic feet. The total area of the shaded blue region is approximately $0.55 in^2$ which is equivalent to 3.55×10^{-4} m^2. Equation 3-1 shows the full derivation from ground reaction force to simulation pressure of 9.9 MPa.

$$P_{simulation} = \frac{F_{expected}}{Area} = \frac{3509\ N}{3.55 * 10^{-4}\ m^2} = 9.884507 * 10^6 Pa \approx 9.9\ MPa \tag{3-1}$$

3.1.5 Parameters and Specifications of FEA Simulation

In order to illustrate the von mises stress distribution of the knee prosthesis, the set up of the FEA simulation is illustrated in Figure 3-7.

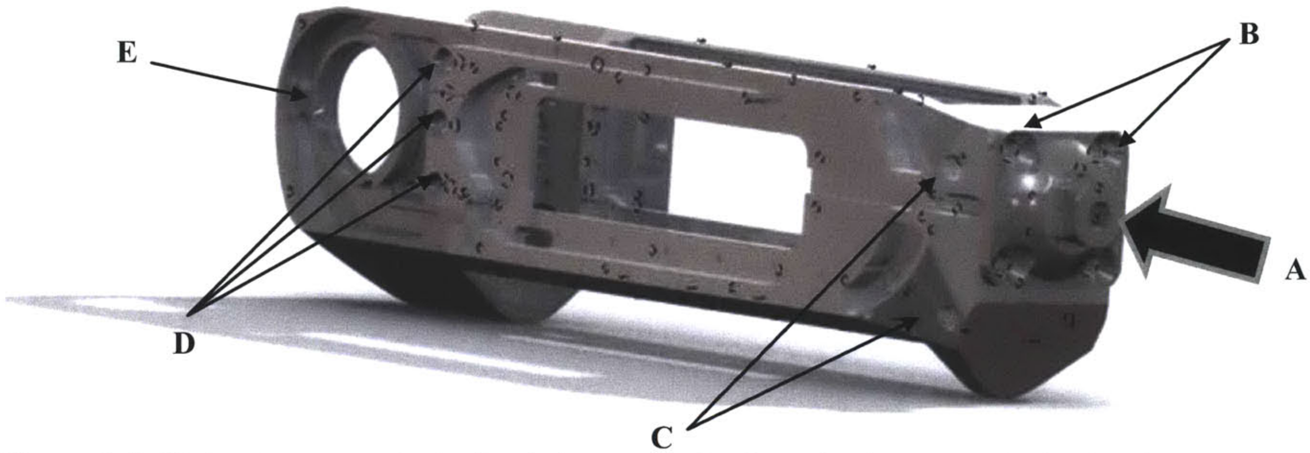

Figure 3-7: Finite element analysis simulation set up for the active knee prosthesis chassis.

A pressure load (A) is applied at the distal plate of the chassis in the axial direction of the prosthesis. The joint (E) is modeled as a fixed component rigidly attached to the overall structure of the knee. The main chassis is connected through bolt connectors. Six M4 countersink-threaded bolts (D) connect the side supports to the knee joint support. Four M4 countersink-threaded bolts (C) connect the side supports to the base support. Four M6 countersink-threaded bolts (B) connect the adapter plate to the base support.

3.1.6 Results

The results of the von-mises stress distribution can be seen in Figure 3-8. An important observation is that even with a safe pressure load corresponding to a patient in the upper limit weight range of 250 lbs, the maximum stress at any point in the chassis does not exceed the yield stress of 7075 Grade Aluminum alloy which has a yield stress of 103 MPa (Matweb, 2011). The maximum stress is approximately 88 MPa and this stress can be found in the base of the distal plate adapter. However, since the distal plate adapter is made of steel rather than aluminum, the part's yield stress is on the order of 250 MPa (Matweb, 2011).

The majority of the chassis parts experience stresses of 10MPa order of magnitude. The thinner cross section portions, regions near the edges, and areas surrounding holes have greater stress levels than other areas. This is an expected outcome since these features cause an abrupt change in the cross sectional area and the stress concentrations increase. The highest area of stress occurs in a very small area near the corner edges of the base proximal to the knee joint. This result is coherent since stress concentrations may appear when a load acts over a very small area and produces higher stresses in the surrounding regions (Gere, 2001).

The areas of high stress concentration should be redesigned to prevent possibilities of yielding and fracture. A method of reducing the stress intensity at these locations would be to provide fillets near sharp edges and corners. Another technique to reduce the stress concentration would be to smooth the surfaces on the inside of holes to prevent cracks from forming (Gere, 2001).

Figure 3-8: Finite element analysis showing the stress distribution of the Revision_1 active knee chassis.

3.2 Initial Weight Reduction Strategy

3.2.1 Preliminary Material Removal

Current knee chassis can structurally support a 250 lbs amputee on level ground walking with a safety factor of two as confirmed by FEA results in the previous section. The next step was to remove material from the chassis such that it can still support the expected safe load without failing. A simple method of material removal was proposed to allow the features of the chassis to retain its mating conditions and maintain its structural integrity. For the side support walls, two millimeters of material were removed. In the top plate, a portion of the part was thinned and circular section were extruded throughout the part. The base plate was pocketed by a volume of 5.73 cc. Table 3-1 shows the reduction in weight through this material removal procedure. The amount of material reduction was experimentally determined to maintain structural integrity in the chassis. The density of 7075 Aluminum is 0.102 lb/in^3 or 2.81 g/cc (Matweb, 2011).

Part	Initial Volume (cc)	Initial Mass(g)	Final Volume(cc)	Final Mass(g)
Knee Joint Support	71.28	200	67.51	190
Side Plate (x2)	67.68	190	61.12	172
Base Plate	32.28	90.7	26.55	74.6
Whole Chassis	238.92	670.7	216.3	608.6

Table 3-1: Reduction in volume and mass of knee chassis after material removal.

From the table, the suggested method of removing material from the knee chassis resulted in a 9.3% reduction in weight of the overall chassis corresponding to 62.1 g. The next step is to determine how the stress distribution of the chassis changed and whether or not it will still be able to support a 250 lbs amputee with a safety factor of two.

3.2.2 Results

The FEA results show that the material removal caused some areas in the knee chassis system to experience stress greater than the yielding stress of 103 MPa. However, most of the chassis experiences stress in the 15-30 MPa magnitude range. There are a few sections near edges and corners which experience such high stress values. These sections occur near the base of the distal adapter plate pyramid and the corner of the knee joint support that contacts the side plates. The distal adapter plate is made of stainless steel rather than 7075 Aluminum so the high stress distribution there does not lead to failure of the part since the highest stress is still below the yield stress of steel which has a value of ~250MPa (Matweb, 2011). The corner of the knee joint support part which comes into contact with the side support plates experience high stress in a very small area of magnitude close to 205 MPa which is still less than 7075 Aluminum's ultimate strength of 221 MPa but greater than the yielding stress of 103 MPa. This increased stress is due to the geometry of the part at that point. Minor revisions in the design or some simple feature machining can remove these points of high stress. Eliminating these sharp edges will smooth out the stress distribution throughout the part and prevent the chassis from yielding or fracture.

The effect of this initial proposed method of material removal resulted in a stress distribution that was within the safe ranges of our design criteria. Based on these results, an improved method of removing material would consider shelling the parts layer by layer uniformly, in order to achieve a relative constant stress distribution and within the yielding stress of the material can be pursued. This procedure, however, would require an automated process that also ensures the feature compatibility of the current design. Furthermore, a more powerful FEA tool could be utilized to optimally set the limit for desired uniform stress and efficiently remove material to obtain the lowest weight reduction while maintaining the structural and functional integrity of the design.

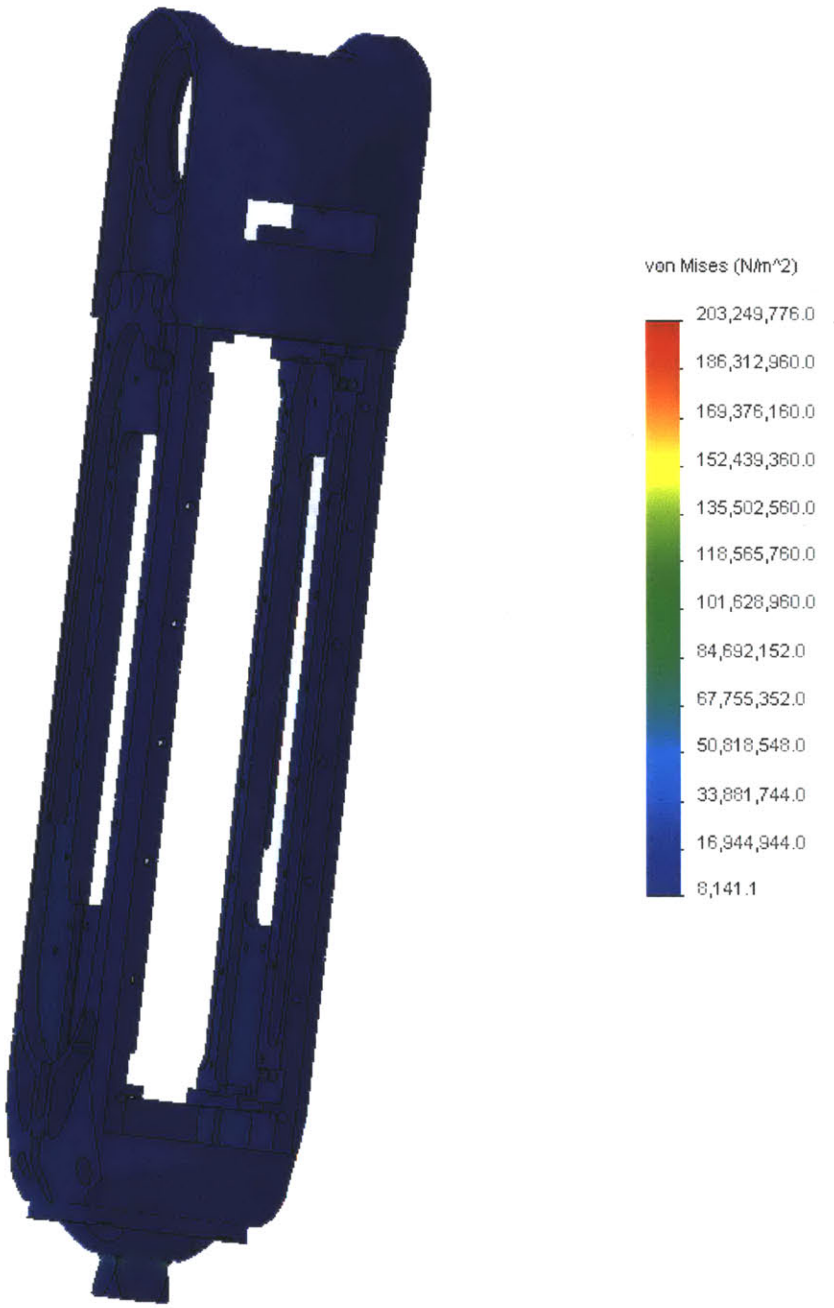

Figure 3-9: Finite element analysis showing the stress distribution of the Revision1 active knee chassis after removing material.

4. Summary and Conclusions

Test Bench Apparatus.

A test bench apparatus was developed to evaluate a biomimeitc active knee prosthesis before subject testing. This apparatus will enable the prosthesis' system characterization for a full model description and will help provide system model parameters for control algorithm development. For this test-bench experimental set-up three major components were designed and analyzed to adapt to Revision_1active knee prosthesis. Finite element analysis verified that each of the three components, (torque sensor adapter, joint lateral mount, and distal mount), satisfied the design criteria based on expected loads. These parts were designed to be structurally rigid and maintain its mechanical integrity during the expected system characterization procedures.

The maximum stress was found to be 44 MPa, 3 MPa, and 13 MPa for the torque sensor adapter, joint lateral mount, and distal mount respectively. The resulting stress levels were all below the yield stress limitation of the material (Al 6061) which has a yield stress of 55 MPa. This result verified that these parts will not experience yielding during characterization experiments under maximum expected loads. The maximum deflection for the joint lateral mount was determined to be 3.0×10^{-5} m which is less than the maximum deflection limit of 3.97×10^{-4} m signifying the component is sufficiently stiff to prevent excessive deformation and failure. The maximum deflection for the distal mount resulted in values under 9.8×10^{-6} m which is less than the maximum deflection limit of 4.23×10^{-4} m established in the design criteria.

Initial Weight Reduction Strategy.

An initial FEA performed on the load bearing chassis of the active knee prosthesis determined it can sustain the maximum forces associated with fast cadence level ground walking of a 250 lbs amputee without the chassis yielding or experiencing fracture. The FEA results showed that the maximum stress levels were below the yield stress of the material. These results verify that the active knee prosthesis structure will not have a structural failure during the human testing evaluations.

After confirming the structural integrity of the active knee chassis, an empirical material removal strategy was proposed. This strategy consisted in uniform material removal on chassis wall and selective extrusions. This material removal was constrained to keep the fastening and functional features of the chassis. After the material removal was performed, a FEA verified the structural integrity of the chassis. A total of 62.1 g of material was removed from the chassis which corresponds to approximately 10 % of the chassis weight and about 2% of the overall prosthesis weight. The negligible weight savings from the proposed strategy suggests that a different method of optimal material removal should be implemented in addition to finding other solutions to minimize prosthetic weight. For this purpose a more powerful FEA tool should be utilized to optimally set the limit for desired uniform stress and efficiently remove material to obtain the lowest weight reduction while maintaining the structural and functional integrity of the design. Some other potential weight saving solutions can be focus on actuator/transmission selection, reduction in the overall number of fasteners, and considering the redesign of the chassis body while maintaining the electromechanical architecture.

References

American Institute of Steel Construction. Specification for Structural Steel Buildings--Allowable Stress Design and Plastic Design. AISC: Chicago, 1989.

Browning, Raymond C., Jesse R. Modica, Rodger Kram, and Ambarish Goswami. *Effects of Adding Mass to the Legs on the Energetics and Biomechanics of Walking*. American College of Sports Medicine. 2007.

Gere, James M. *Mechanics of Materials*. Pacific Grove, CA: Brooks/Cole. 2001.

Huang, G. F., Chou, Y. L. and Su, F. C. *Gait analysis and energy consumption of below-knee amputees wearing three different prosthetic feet. Gait Posture*. 2000.

James, U. *Oxygen uptake and heart rate during prosthetic walking in healthy male unilateral above-knee amputees. Scand J Rehabil Med* 5: 71-80. 1973.

Johansson J., Sherrill D., Riley P., Paolo B., Herr H. "A Clinical Comparison of Variable-Damping and Mechanically-Passive Prosthetic Knee Devices", *Am l of Phy Med & Rehabn.* 84(8), pp 563-575). 2005.

Martinez-Villalpando, Ernesto C. *Agonist-antagonist active knee prosthesis: A preliminary study in level-ground walking*. Journal of Rehabilitation Research & Development. 2009.

Martinez-Villalpando, E.C., Weber J., Elliott, G., and Herr, H.. "*Design of an Agonist-Antagonist Active Knee Prosthesis*". Proceedings of IEEE BIORobotics Conference, Scottsdale, Arizona, October 19-22, 2008.

Martinez-Villalpando, E.C., Weber J., Elliott, G., and Herr, H 2008, "*Biomimetic Prosthetic Knee using Antagonistic Muscle-Like Activation* " ASME International Mechanical Engineering Congress and Exposition (MIECE), Boston, MA, 2008.

Marsh, Robert L., David J. Ellerby, Havalee T. Henry, and Jonas Rubenson. *Energetic costs of trunk and distal-limb loading during walking and running in guinea fowl Numida meleagris.* The Journal of Experimental Biology. 2006.

Material Property Data. *MatWeb* Automation Creations, Inc. Blacksburg, VA, 2011. http://www.matweb.com.

Waters, R.L. , J Perry, D Antonelli, and H Hislop. *Energy cost of walking of amputees:the influence of level of amputation*. The Journal of Bone & Joint Surgery. 1976

Whittle, Michael W. *Gait Analysis: an introduction Third Edition.* Butterworth Heinemann, 2003.

Winter, David A. *The Biomechanics and Motor Control of Human Gait: Normal, Elderly, and Pathological Second Edition.* University of Waterloo Press. 1991.

Appendix A - Engineering Drawings

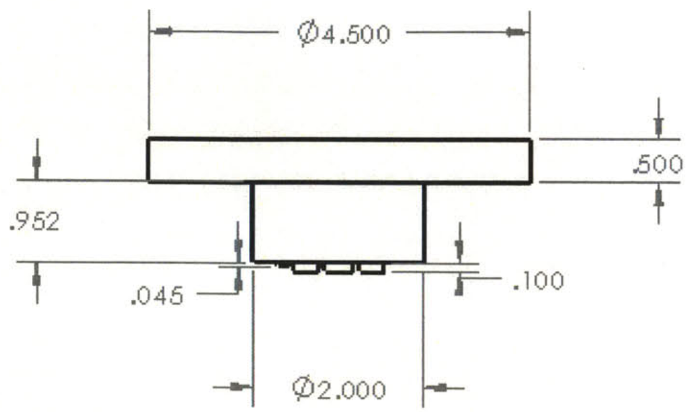

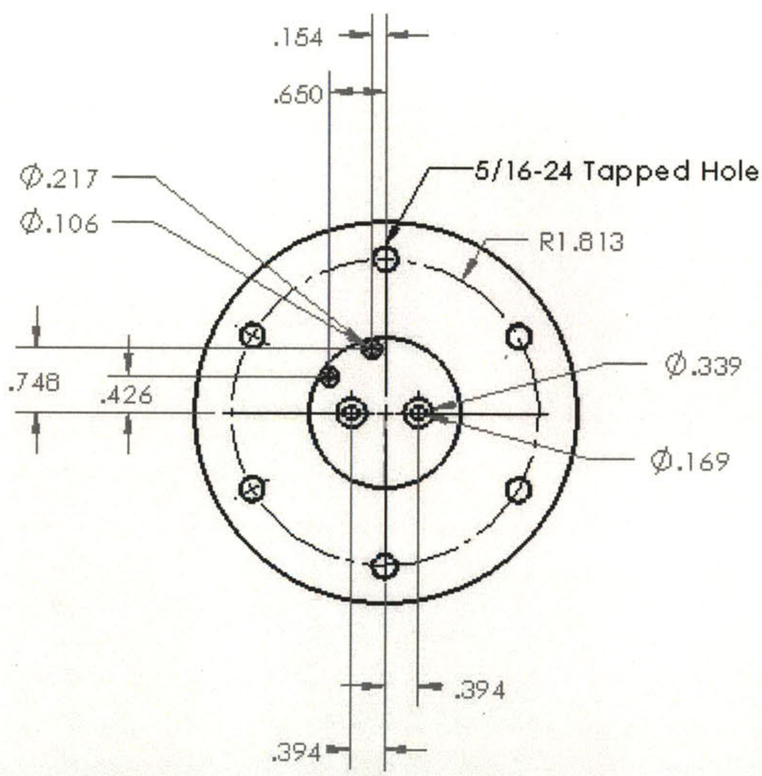

NOTE
1. All Diminensions are in inches

Torque Sensor Adapter

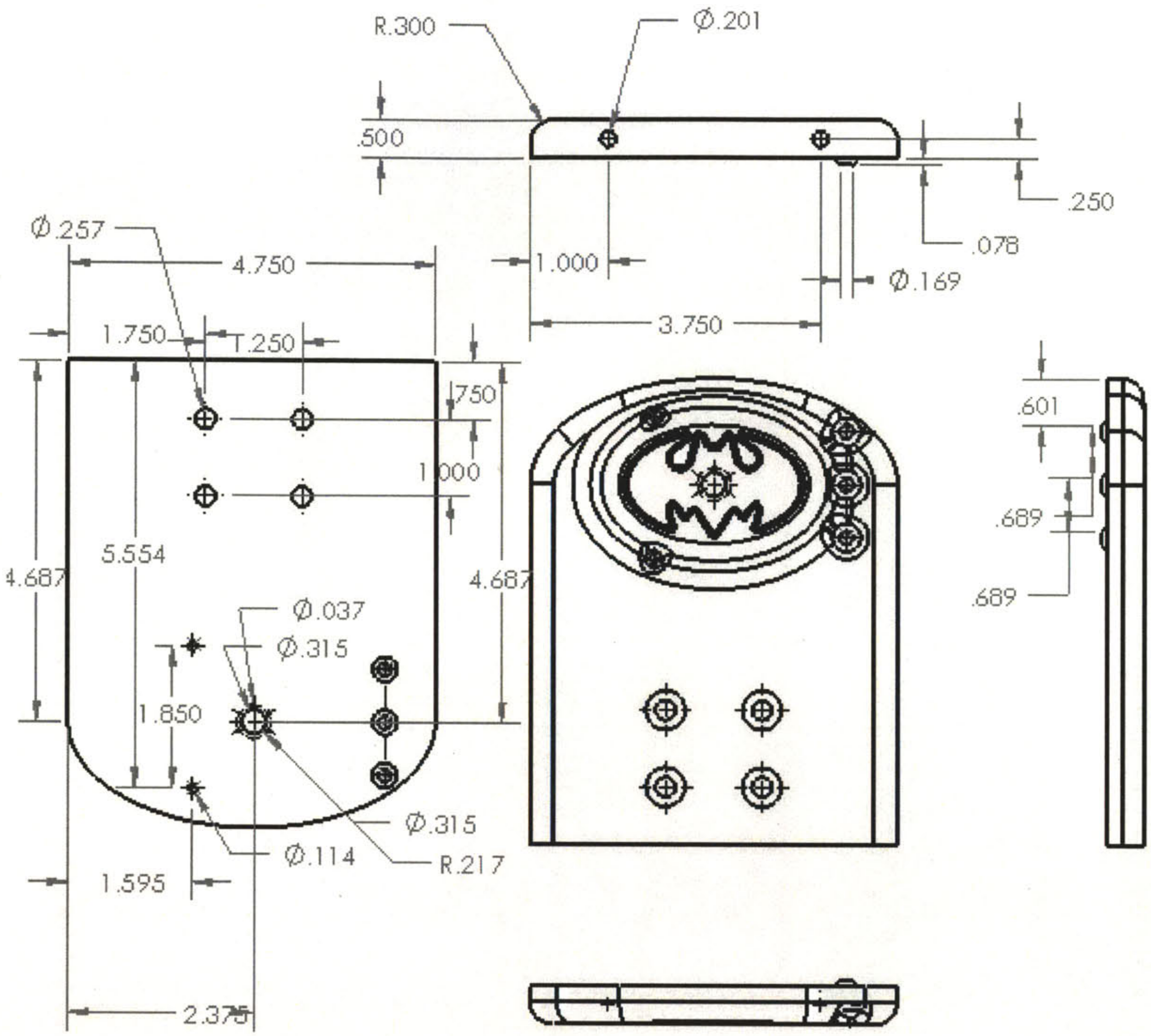

NOTE
1. All Dimensions are in inches.

Joint Lateral Mount

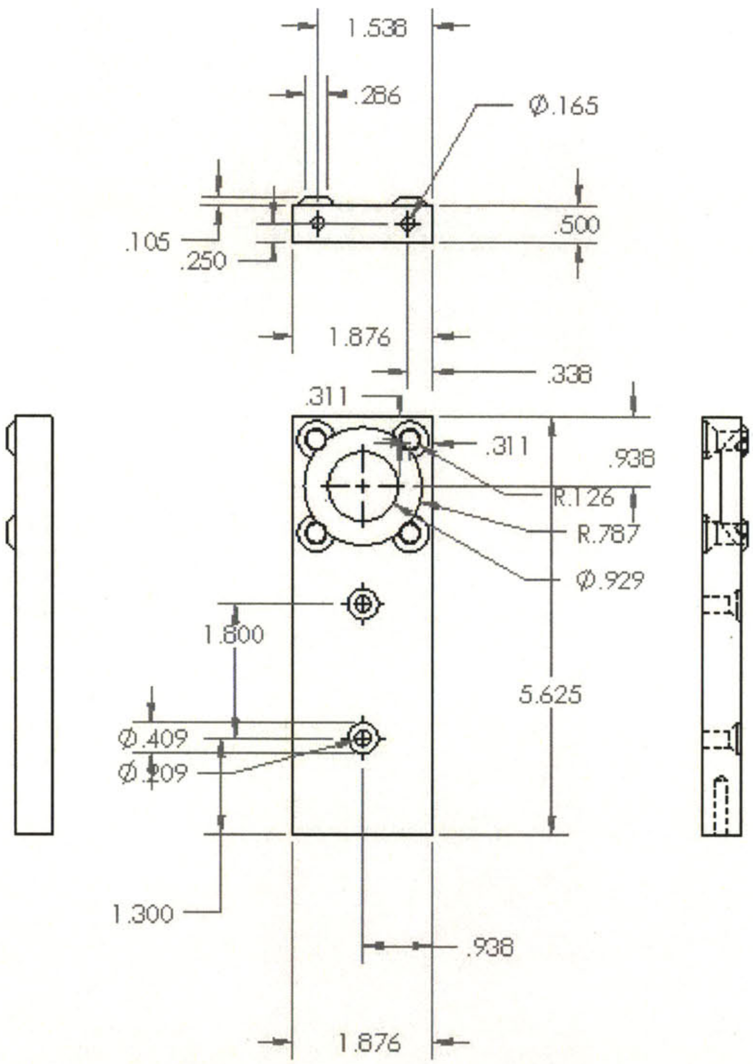

NOTE
1. All Dimensions are in inches.

Distal Mount

Appendix B - Finite Element Results

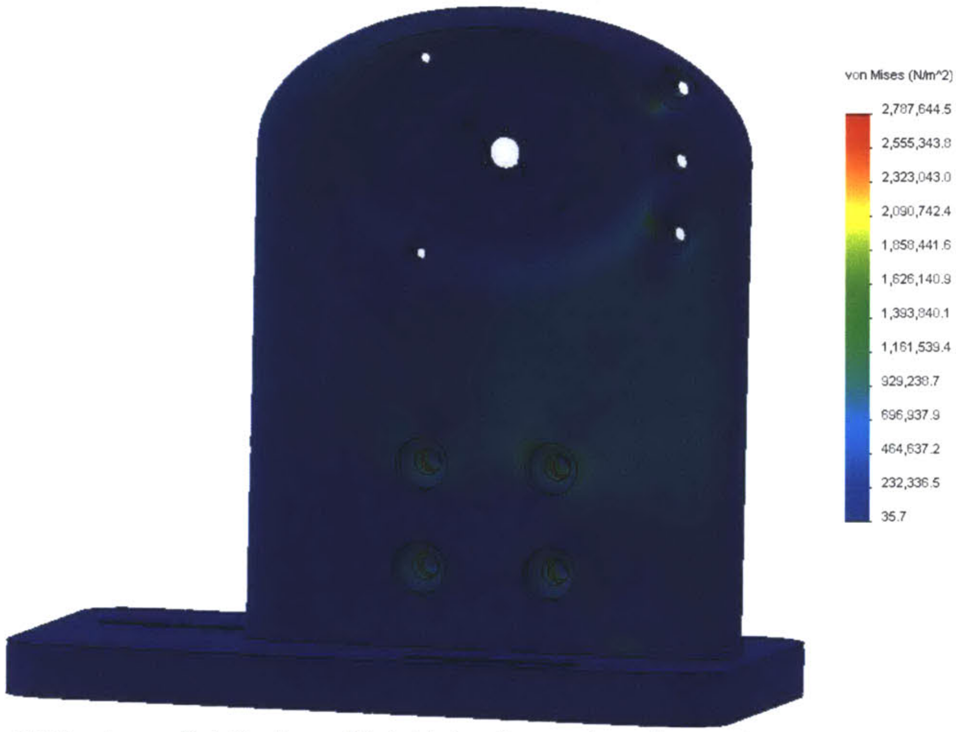

Figure B-1: FEA, stress distribution of joint lateral mount wedge system.

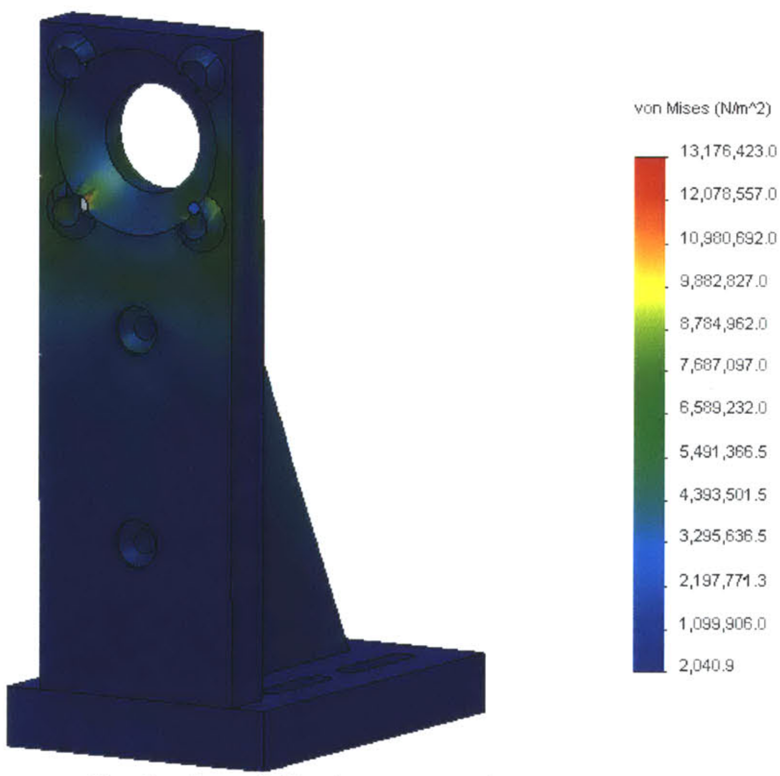

Figure B-2: FEA, stress distribution of distal mount wedge system.